Electron correlations in stripe phases for doped antiferromagnets

Dariusz Góra and Krzysztof Rościszewski
Institute of Physics, Jagellonian University, Reymonta 4, PL-30059 Kraków, Poland

Andrzej M. Oleś
Institute of Physics, Jagellonian University, Reymonta 4, PL-30059 Kraków, Poland
and Max-Planck-Institut für Festkörperforschung, Heisenbergstrasse 1, D-70569 Stuttgart, Federal Republic of Germany
(Received 4 March 1999; revised manuscript received 11 May 1999)

We present the charge and magnetization density distribution in various stripe phases obtained for two-dimensional models of correlated electrons solved within the Hartree-Fock approximation and a variational *local ansatz*. Apart from the Hubbard model with local Coulomb interaction U, we investigate its two extensions by adding either static Peierls electron-lattice coupling, or the correlated hopping term in the so-called Hirsch model. It has been found that the stripe ordering is robust and occurs in underdoped ($\delta=1/8$) and overdoped ($\delta=1/4$) systems. At intermediate values of U in underdoped systems ($\delta=1/8$) local correlations stabilize the vertical (01) antiferromagnetic domains, separated by nonmagnetic domain walls filled by one doped hole per two wall atoms. A stripe phase with the same size of magnetic domains and an increased filling of one hole per one wall atom is stable for overdoped ($\delta=1/4$) systems. At larger values of U, both structures are replaced by more extended magnetic domain walls oriented along the (11) direction. These findings agree qualitatively with the experimental results. [S0163-1829(99)13733-0]

I. INTRODUCTION

Nonhomogeneous charge and spin ordering in real space, so-called *stripe phases*, attracted much attention due to their possible role in the high-temperature superconductivity of the cuprates. In contrast to the high-temperature superconductivity itself, the stripe instability of the effective Hubbard model describing a normal phase of the cuprates was first predicted in the theory within Hartree-Fock (HF) calculations on finite clusters with periodic boundary conditions,[1] and later verified experimentally. The theoretical discovery was soon followed by the experimental observation of incommensurate spin correlations in $La_{2-x}Sr_xCuO_4$ by neutron scattering experiments.[2] However, a clear identification of a stripe phase was possible only more recently in $La_{1.6-x}Nd_{0.4}Sr_xCuO_4$, where the stripe structures are pinned.

Neutron scattering experiments[3–5] performed on $La_{1.6-x}Nd_{0.4}Sr_xCuO_4$ demonstrate the existence of the stripe phases, with antiferromagnetic (AF) spin domains, separated by charged domain walls. Neutron diffraction measurements on single crystals with the hole doping ratio $\delta\simeq 1/8$ revealed the existence of two kinds of incommensurate superlattices peaks.[4] In the reciprocal space the magnetic peaks are satellites of the AF Bragg reflection at $\mathbf{k}=(\pi,\pi)$; they are displaced along the (10) and (01) directions to $\mathbf{k}=[\pi(1\pm 2\eta),\pi]$ and $\mathbf{k}=[\pi,\pi(1\pm 2\eta)]$, respectively, while at the same time the charge-order x-ray satellite diffraction peaks are displaced by 4η with respect to the peak at $\mathbf{k}=(0,0)$ found for a uniform distribution. Experiments at low temperature for $La_{1.6-x}Nd_{0.4}Sr_xCuO_4$ showed that $\eta\simeq\delta$ at small doping $\delta\leqslant 1/8$, while η is almost constant at higher doping.[5]

The appearance of peaks in neutron scattering at incommensurate positions points out toward two possibilites: either (i) there are two types of twin domains, half of them with the modulation wave vector aligned along the x axis and the other half with the modulation along the y axis or (ii) only a single type of domain with the modulation both along the x and the y axes is formed. The experiments are usually interpreted within the first scenario, which is also supported by numerous theoretical papers devoted to the study of striped phases.[1,6–10]

So far, the stripe phases were found numerically using the two-dimensional (2D) Hubbard (or t-J) model in the HF calculations,[1,6,7] using the density matrix renormalization group (DMRG),[8] in slave boson calculations,[9] and in the dynamical mean field theory (DMFT).[10] All these calculations point out a universal instability of the Hubbard model: the stripe phases with the domain walls along one of the main directions, either (10) or (01), called also for convenience vertical stripes [which refer to the domain walls along the (01) direction], were found independently of the applied method at intermediate values of U/t, where U is a local Coulomb interaction, and t is a nearest-neighbor hopping element.

Experimentally, the domain walls found at $\delta=1/8$ doping occur at every fourth vertical line which implies that the density of doped holes is one doped hole per two atoms of the domain wall.[3,4] Such stripes are called half-filled stripes,[7] in contrast to the stripes with one hole per domain wall atom, so-called filled stripes, observed in the nickelates.[11] Both types of stripe phases were found in the HF calculations,[7] but it turned out to be difficult to stabilize the ground state with half-filled domain walls, as observed in the cuprates.[3] Therefore, it is necessary to go beyond the HF approach and include explicitly the effects of electron correlation. Here we address three important questions related to the stability of stripe phase in the presence of electron correlations: (i) whether electron correlations are stabilizing the stripe solutions, (ii) whether the half-filled domain walls are more stable than other stripe solutions, and finally (iii) whether

new types of stripe phases could be stabilized by electron correlations. We investigate these questions using a local ansatz (LA) method, introduced some time ago to treat local correlations in quantum chemistry,[12] and used also successfully in various models of correlated electrons on a lattice.[13–15]

In this contribution we will not attempt to understand the nature of the stripe quantum fluid.[16,17] Instead, we will concentrate on a simpler question to what extent the stripe instability is universal and occurs for different Hamiltonians with strong on-site Coulomb interactions. We will argue that this universality supports rather the frustrated phase separation mechanism[18] over a Fermi-surface instability,[1,6] in agreement with recent experiments.[3,4] Therefore, we investigate three different Hamiltonians of the Hubbard type. (i) First, we study the standard single-band Hubbard Hamiltonian, being a generic model of correlated electrons. (ii) Second, we included in this model static Peierls coupling to the lattice. This extension of the Hubbard model was motivated by the idea that nonhomogeneous solutions with doped holes localized on domain walls, as found in striped phases, might be stabilized by accompanying them static lattice distortions. The same model was considered earlier in the HF studies of Ref. 7, and here we investigate the corrections which follow from the correlation effects. (iii) Finally, we introduce also the correlated hopping term which depends on the actual occupancy of the involved bond by the electrons of the opposite spin, considered in the so-called Hirsch model.[19,20] Here we investigate whether such terms change significantly the stripe stability. Altogether, we believe that these three models may be considered as effective models for the low-energy physics of realistic high temperature superconductors and could be justified by an appropriate mapping of the realistic electronic models onto a single-band Hamiltonian of Hubbard type.[21]

The paper is organized as follows. The models of correlated electrons in a nondegenerate band are presented in Sec. II. In the same section we introduce the LA method to treat local correlations, and define the characteristic functions used to describe the numerically obtained charge and spin density distributions in stripe phases. The numerical results for two doping levels $\delta=1/8$ and 1/4 are presented and discussed in Sec. III. A short summary and conclusions are given in Sec. IV.

II. DESCRIPTION OF STRIPE PHASES

A. Models of correlated electrons

As already mentioned, we study the stripe phases in a nondegenerate band with local Coulomb interaction U, using finite clusters described by three Hamiltonians: the single-band Hubbard Hamiltonian

$$H_1=-t\sum_{ij\sigma}\ c_{i\sigma}^{\dagger}c_{j\sigma}+U\sum_{i}\ n_{i\uparrow}n_{i\downarrow}, \tag{1}$$

the single-band Hubbard Hamiltonian which includes the so-called static phonons[7]

$$H_2=-t\sum_{ij\sigma}\ (1+\alpha u_{ij})c_{i\sigma}^{\dagger}c_{j\sigma}+U\sum_{i}\ n_{i\uparrow}n_{i\downarrow}+\tfrac{1}{4}K\sum_{ij}\ u_{ij}^{2}, \tag{2}$$

and, finally, the Hirsch Hamiltonian[19,20]

$$H_3=-t\sum_{ij\sigma}\ [1-\beta(1-n_{i,-\sigma}-n_{j,-\sigma})]c_{i\sigma}^{\dagger}c_{j\sigma}+U\sum_{i}\ n_{i\uparrow}n_{i\downarrow}. \tag{3}$$

Here $c_{i\sigma}^{\dagger}(c_{i\sigma})$ are creation (annihilation) operators for an electron with spin $\sigma=\uparrow,\downarrow$ at site i, and $n_{i\sigma}=c_{i\sigma}^{\dagger}c_{i\sigma}$ are electron number operators. The hopping elements are finite, $t_{ij}=-t$, on the bonds (ij) which connect nearest neighbors. The correlated hopping matrix element $\propto\beta$ describes a difference in electron hopping amplitudes between singly and doubly occupied sites.[19,20] Finally, K in Eq. (2) stands for the elastic energy and u_{ij} are fractional changes of the (ij) bondlength between nearest-neighbor sites i and j with respect to its (equilibrium) reference value.[22]

We investigated also the consequences of the correlated hopping term by taking a single representative value of $\beta=0.3$ in the Hirsch model (3). Therefore, the hopping element in an empty band amounts to $t(1-\beta)=0.7t$. Using the independent electron picture, the hopping increases when at least one of the sites i or j, is occupied by an electron with an opposite spin, and for the present choice of parameters one finds again the effective hopping t within the HF approximation at half filling. However, in the strongly correlated regime where the double occupancies are excluded, the correlation effects reduce the hopping to $(1-\beta)t$. The Hamiltonian (3) serves to address the problem of nonhomogeneity from the point of view of possible ''Coulomb instabilities.'' We note that a similar problem was recently addressed in the presence of long-range Coulomb interactions within the slave-boson technique.[9]

We considered 2D square clusters containing up to $N=64$ sites with periodic boundary conditions, i.e., using an 8×8 supercell, with hole doping $\delta=1-n$ away from half filling $(n=1)$, where n is an electron density. Let us remark on inherent (but well understood) limitations of modelling an infinite solid by finite cluster calculations. In this respect the used periodic boundary conditions ensure that influence of finite size effects (versus bulk properties) is minimized. The actual number of holes in the cluster is $N_h=N\delta$, where N is the number of sites. For convenience we choose $t=1$ as an energy unit, and vary the Coulomb interaction U in the range of $3<U/t<10$ which includes the typical values for the cuprate superconductors, $8\leqslant U/t\leqslant10$. The other parameters of the Hamiltonian with static phonons (2) were assumed to be the same as in the previous HF study:[7] $K/t=18$ and $\alpha=3$.

The model Hamiltonians (1), (2), and (3) are first solved self-consistently within the standard nonhomogeneous HF approximation, where the on-site interactions are replaced by one-particle terms

$$n_{i\uparrow}n_{i\downarrow}\simeq n_{i\uparrow}\langle n_{i\downarrow}\rangle+\langle n_{i\uparrow}\rangle n_{i\downarrow}-\langle n_{i\uparrow}\rangle\langle n_{i\downarrow}\rangle. \tag{4}$$

As we do not consider spin spirals, we use the simplest close-shell version of the HF method with a product of two Slater determinants for up and down spins separately. Such solutions serve as reference states $|\Phi_0\rangle$ for calculating the correlated states, as described in Sec. II B.

The calculations performed for the Hubbard Hamiltonian with phonons (2) use an approximate procedure as introduced in the Appendix. Unfortunately, a rigorous inclusion

of the phonon (kinetic and potential) energies is a difficult task. So far, only a limited progress was achieved in spite of numerous attempts (a typical recent example is given in Ref. 23). Therefore, we limit ourselves to the static phonons, and follow the procedure introduced by Dobry *et al.*[24] and by Zaanen and Oleś.[7]

B. Local correlations

The electronic correlations were treated using a *nonhomogeneous* variational method, known as a local ansatz.[12,13,15] This method captures the leading contribution to the correlation energy in the present systems with nonhomogeneous density distribution of doped holes. It follows from the form of model Hamiltonians (1)–(3) that it suffices to introduce only the on-site local correlation operators in oder to determine the ground state energy with reliable accuracy. Thus, the wave function up to lowest order is equivalent to that introduced by Gutzwiller for the Hubbard model.[25] Here we avoid the simplifications introduced by the Gutzwiller approximation, and use an exponential ansatz for the correlated ground state[12,13]

$$|\Psi_0\rangle = \exp\left(-\sum_i \eta_i O_i\right)|\Phi_0\rangle, \tag{5}$$

where

$$O_i = n_{i\uparrow}n_{i\downarrow} - \langle n_{i\uparrow}\rangle\langle n_{i\downarrow}\rangle \tag{6}$$

are the local operators and η_i are the corresponding variational parameters. The averages $\langle\cdots\rangle$ are determined, as usually, by averaging over the HF ground state function $|\Phi_0\rangle$. By construction the local operators describe the correlations which go *beyond* the HF state, and $\langle O_i\rangle = 0$. For convenience, we use also a shorter notation for the one-particle averages, $\overline{n_{i\uparrow}} = \langle n_{i\uparrow}\rangle$, and define the local doped hole density in the correlated ground state $|\Psi_0\rangle$ as follows:

$$n_{hi,\mathrm{LA}} = \frac{\langle\Psi_0|1-(n_{i\uparrow}+n_{i\downarrow})|\Psi_0\rangle}{\langle\Psi_0|\Psi_0\rangle}. \tag{7}$$

The HF ground state function $|\Phi_0\rangle$ describes the reference state with magnetic order and local order parameters

$$m_{i,\mathrm{LA}} = \frac{|\langle\Psi_0|(1/2)(n_{i\uparrow}-n_{i\downarrow})|\Psi_0\rangle|}{\langle\Psi_0|\Psi_0\rangle}, \tag{8}$$

defined by the breaking of symmetry with respect to the zth spin component $S_i^z = \frac{1}{2}(n_{i\uparrow}-n_{i\downarrow})$. This construction allows us to use a closed-shell version of the HF wave function $|\Phi_0\rangle$ with the factorization of the Slater determinant into up-spin and down-spin parts.[26]

The variational parameters η_i are fixed by minimizing the total energy in the correlated ground state

$$E_0 = \frac{\langle\Psi_0|H_m|\Psi_0\rangle}{\langle\Psi_0|\Psi_0\rangle}, \tag{9}$$

where $H_m (m=1,2,3)$ is one of the Hamiltonians introduced in the previous section, and the values of the variational parameters η_i^0 correspond to the global minimum. After expanding the exponential factors in the wave functions $|\Psi_0\rangle$ (5) up to linear order in η_i, they can be easily determined by minimizing the energy (9),[12]

$$\boldsymbol{\eta}^0 = \hat{a}^{-1}\mathbf{b}, \tag{10}$$

$$E_0 = E_{\mathrm{HF}} - \mathbf{b}\boldsymbol{\eta}^0, \tag{11}$$

where the elements of the vector $\mathbf{b}$ and matrix $\hat{a}$ are defined as follows:

$$b_i = \langle O_i H_m\rangle, \tag{12}$$

$$a_{ij} = \langle O_i(H_{m,\mathrm{HF}} - E_{\mathrm{HF}})O_j\rangle, \tag{13}$$

and E_{HF} is the HF energy calculated from the HF Hamiltonian $H_{m,\mathrm{HF}}$, which is obtained from H_m. The above equation is valid provided that any third and higher order fluctuations such as $\sim\langle(n_{i\uparrow}-\overline{n_{i\uparrow}})^3\rangle$ are small and can be neglected.[12] This condition is well satisfied in the symmetry-broken states with AF order considered in the present study. More details on the energy minimization in the LA method may be found in Refs. 13 and 14.

As an example, we give below explicit formulas for $\mathbf{b}$ and $\hat{a}$ for the Hubbard Hamiltonian, either without [Eq. (1)] or with [Eq. (2)] static phonons,

$$b_i = U\sum_s \{\langle n_{i\uparrow}n_{s\uparrow}\rangle\langle n_{i\downarrow}n_{s\downarrow}\rangle - \overline{n_{i\uparrow}}\,\overline{n_{s\uparrow}}\langle n_{i\downarrow}n_{s\downarrow}\rangle - \overline{n_{i\downarrow}}\,\overline{n_{s\downarrow}}\langle n_{i\uparrow}n_{s\uparrow}\rangle + \overline{n_{i\uparrow}}\,\overline{n_{s\uparrow}}\,\overline{n_{i\downarrow}}\,\overline{n_{s\downarrow}}\}, \tag{14}$$

$$a_{ij} = \langle n_{i\downarrow}n_{j\downarrow}\rangle\sum_{M\mu}(\varepsilon_\mu^\uparrow - \varepsilon_M^\uparrow)v_{iM}^\uparrow v_{i\mu}^\uparrow v_{jM}^\uparrow v_{j\mu}^\uparrow + \langle n_{i\uparrow}n_{j\uparrow}\rangle \times\sum_{M\mu}(\varepsilon_\mu^\downarrow - \varepsilon_M^\downarrow)v_{iM}^\downarrow v_{i\mu}^\downarrow v_{jM}^\downarrow v_{j\mu}^\downarrow, \tag{15}$$

where the subscripts M and μ run over occupied and unoccupied (virtual) HF one-particle states, respectively. In order to distinguish them from lattice site indices we use either capitals (for occupied states) or Greek characters (for unoccupied states). The HF eigenenergies are ε_M and ε_μ, respectively, and v_{iM}^σ and $v_{i\mu}^\sigma$ label the component i of the corresponding eigenvectors for spin σ. Let us remind here that the (real) unitary transformation from electron creation (annihilation) operators defined on lattice sites to the electron creation (annihilation) operators corresponding to occupied and virtual one-particle HF states is realized by the matrix constructed from the eigenvectors $\{v_M^\sigma, v_\mu^\sigma\}$. For the Hirsch Hamiltonian H_3 one finds that Eq. (15) does not change, while the b_i elements may be straightforwardly derived and satisfy a slightly modified Eq. (14).

The ground-state energies of the obtained correlated solutions, $E_0(\delta)$, depend on the size of the cluster and on the doping level δ. As a measure of stability of various textures it is convenient to introduce the energy gain per one doped hole,[7]

$$E_h = \frac{1}{N_h}[E_0(\delta) - E_0(\delta=0)], \tag{16}$$

where $E_0(\delta=0)$ is the reference energy of the undoped AF phase. As the ground-state energy we use either the energies found within the LA method (9), as explained above, or the HF energy as introduced before in Ref. 7.

C. Charge and spin structure factors

For the characterization of charge and magnetization distribution in the correlated states $\{|\Psi_0\rangle\}$ it is convenient to introduce two functions which are directly measured in elastic coherent scattering experiments $C(\mathbf{k})$ and $S(\mathbf{k})$. First of them, the x-ray elastic scattering function $C(\mathbf{k})$ is a Fourier transform of the density distribution

$$C(\mathbf{k})=\frac{1}{N}\sum_{ij}\langle n_i\rangle\langle n_j\rangle e^{i\mathbf{k}(\mathbf{R}_i-\mathbf{R}_j)}, \tag{17}$$

where $\mathbf{R_i}$ are the real space lattice vectors. The second function $S(\mathbf{k})$ is related to the elastic neutron unpolarized spin scattering. The measured double differential cross section is proportional to the neutron scattering function[27]

$$\mathcal{F}(\mathbf{k})=\sum_{\alpha,\beta}\left(\delta_{\alpha\beta}-\frac{k_\alpha k_\beta}{k^2}\right)S^{\alpha\beta}(\mathbf{k}), \tag{18}$$

where

$$S^{\alpha\beta}(\mathbf{k})=\frac{1}{N}\sum_{ij}\langle S_i^\alpha\rangle\langle S_j^\beta\rangle e^{i\mathbf{k}(\mathbf{R}_i-\mathbf{R}_j)} \tag{19}$$

describes the spin structure and k_α is the α component of the scattering vector. We note that for the stripe states considered in the present paper one finds $\langle S_i^x\rangle=\langle S_i^y\rangle=0$ (assuming the magnetization direction along the z axis),[26] so the neutron scattering function may be further simplified. We use below $S(\mathbf{k})=S^{zz}(\mathbf{k})$ for the only nonvanishing component of the spin-spin correlation function.

We introduce also after White and Scalapino[8] a different way of describing the domain wall structure by the charge

$$n_h(l_x)=1-\frac{1}{L_y}\sum_{l_y=1}^{L_y}\langle n_{(l_x,l_y),\uparrow}+n_{(l_x,l_y),\downarrow}\rangle \tag{20}$$

and spin

$$S_\pi(l_x)=\frac{1}{L_y}\sum_{l_y=1}^{L_y}(-1)^{l_x+l_y}\frac{1}{2}\langle n_{(l_x,l_y),\uparrow}-n_{(l_x,l_y),\downarrow}\rangle, \tag{21}$$

correlation functions in real space. Here we use an explicit notation for the site indices $\mathbf{l}=(l_x,l_y)$ in terms of two coordinates. Equations (20) and (21) are well designed to analyze vertical domain walls, as they describe the changes of the charge and magnetization distribution in the x direction perpendicular to such domain walls. Analogous formulas with the summations performed along one of the diagonal directions capture the relevant density changes for the diagonal domain walls.

We have verified that the charge and magnetization distribution for particular stripe phases do not change significantly in the presence of electron correlations. However, the stripe phase found in the ground state depends on the actual value of the local Coulomb interaction U/t, as presented in the next section.

III. NUMERICAL RESULTS

We considered 2D square clusters containing up to $N=64$ sites with periodic boundary conditions, i.e., an 8×8 supercell, with hole doping $\delta=1-n$ away from half-filling ($n=1$), where n is an electron density. Let us remark on inherent (but well understood) limitations of modelling an infinite solid by finite cluster calculations. In this respect the used periodic boundary conditions ensure that influence of finite size effects (versus bulk properties) is minimized.

We have investigated the ground states of the Hamiltonians (1)–(3) by performing self-consistent calculations for the 8×8 clusters with periodic boundary conditions for the undoped systems and for two doping levels $\delta=0.125$ and $\delta=0.25$. They correspond to the underdoped and overdoped regime of the high-temperature superconductors, respectively. In the undoped case the ground state is homogeneous with AF long-range order, independently of the assumed narrow-band Hamiltonian (1)–(3). In contrast, in the doped systems a rich variety of textures can be systematically investigated by varying the initial conditions and the value of Coulomb interaction U. We have identified several new phases as compared with the earlier HF study,[7] some of them stabilized by the electron correlations. Below we present only the most stable solutions found for two investigated doping levels.

A. Underdoped systems, $\delta=0.125$

Let us concentrate first on the underdoped systems with $\delta=0.125$. The most typical solutions obtained in this case with the increasing value of Coulomb interaction U/t are presented in Fig. 1: two vertical half-filled domain walls [Fig. 1(a)], two types of the half-filled walls with density alternation [Figs. 1(b) and 1(c)], and two extended diagonal walls [Fig. 1(d)]. These structures reproduce a generic crossover from the vertical (01) to diagonal (11) walls with increasing Coulomb interaction, as reported in the early HF studies.[1,6] However we emphasize that the structure depicted in Fig. 1(d) although being more spacially extended has lower energy than the simpler phase with the doped holes located on single lines along the (11) direction. The most stable stripe structures shown in Fig. 1 are globally stable for particular Coulomb interaction U/t, but frequently other stripe phases are locally stable, with only small energy difference with respect to the determined ground state. Therefore, while the regions of stability of various solutions might still change in a more accurate treatment, one expects that the phase separation into (doped) hole-rich and hole-poor regions, similar to that established for the t-J model,[18,28] occurs in the present model systems, with the doped holes ordered along particular lines.

As seen in Fig. 1 and in the charge density maps for these four typical structures (see also Figs. 2), the regions of increased doped holes concentration separate AF domains with large magnetic moments and with small almost nonmodulated hole density. Concerning the hole density distribution,

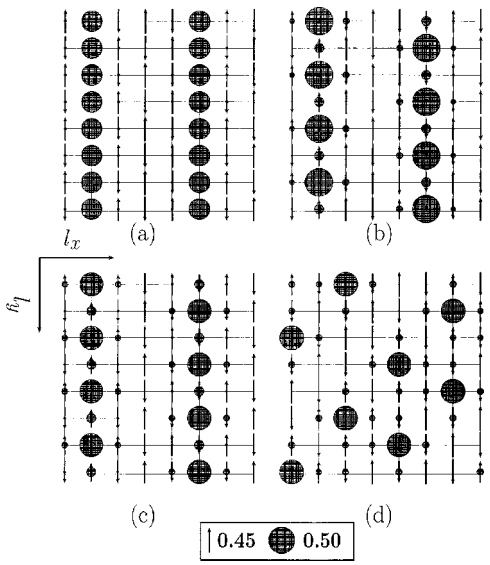

FIG. 1. The most typical stripe phases as obtained at doping $\delta = 0.125$ using LA method: (a) a half-filled nonmagnetic (01) domain wall (Hubbard model, $U = 10t$), (b) two weakly ferromagnetic (FM) half-filled (01) domain walls with charge alternation (Hubbard model with static phonons, $U = 9.25t$), (c) two FM half-filled (01) structures with quadrupling of charge and spin ordering within a single AF domain (Hirsch model, $U = 6.5t$), (d) diagonal extended walls with FM order and isolated holes (Hirsch model, $U = 9.5t$). The diameter of the grey circles is proportional to the hole density $n_{hi,\mathrm{LA}}$ (7), and the length of the arrows is proportional to $\langle S_i^z \rangle_{\mathrm{LA}}$ (8) according to the scales shown at the figure bottom.

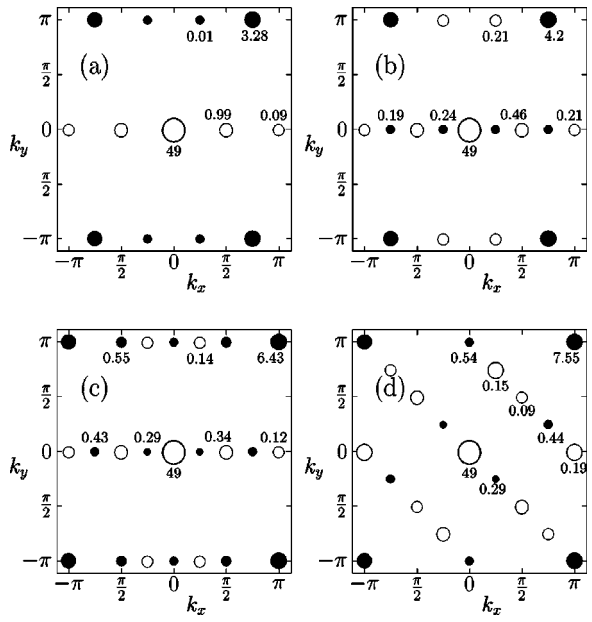

FIG. 2. The magnetic and charge ordering obtained in reciprocal space for doping $\delta = 0.125$ in an 8×8 cluster within the LA method: the magnetic peaks (full circles) correspond to spin structure (19) seen in neutron elastic scattering function $S(\mathbf{k})$; the charge peaks (open circles) give the charge distribution (17) as observed in x-ray scattering function $C(\mathbf{k})$. The numbers accompanying the circles indicate the peaks intensities. Different panels represent the most stable solutions shown in Fig. 1: (a) striped phase with two half-filled nonmagnetic (01) domain walls, $U = 10t$ [Fig. 1(a)], (b) striped phase with two half-filled (01) domain walls with charge alternation, $U = 9.5t$ [Fig. 1(b)], (c) two half-filled FM stripes within a single AF domain, $U = 6.5t$ [Fig. 1(c)], (d) polarons in the (11) extended stripes of increased hole density within a single AF domain, $U = 9.5t$ [Fig. 1(d)].

the half-filled walls of Fig. 2(a) have a uniform density along the wall, while the other three structures of Fig. 1 which occur at higher values of U/t are characterized by the spacial modulation of doped hole density, either along the (01) direction [Figs. 2(b) and 2(c)], or along the (11) direction [Fig. 2(d)].

The obtained magnetic textures may be classified into two types of solutions: the domain walls of Figs. 1(a) and 1(b) separate two different AF domains, while the remaining structures [shown in Figs. 1(c) and 1(d)] correspond to a single domain with a nonhomogeneous distribution of doped holes. This difference is best seen in the distribution of maxima in the magnetic structure factor $S(\mathbf{k})$, shown in Figs. 2(a)–2(d). One finds strong maxima at the values of $\mathbf{k} = (\pm 3\pi/4, \pm \pi)$ for the structures with two domain walls [Figs. 1(a) and 1(b)], while for the structures with a single AF domain the strongest peak at $\mathbf{k} = (\pi, \pi)$ is accompanied by some weaker satellites [Figs. 1(c) and 1(d)]. The same applies to the spin-bag structure stable at small values of U/t (not shown), with an extended region of increased hole density and reduced AF order. Looking at the reciprocal space pattern we conclude that such spin-bag structure corresponds to the intersecting grid of diagonal walls, i.e., along (11) and $(1\bar{1})$ directions. We further note that only the structures with the magnetic maxima displaced from the AF value of $\mathbf{k} = (\pi, \pi)$ agree well with the experimental observations.[3–5]

The numerical results obtained for the energy of different textures are summarized in Fig. 3. First of all, the collected data allow us to conclude that the tendency to form vertical walls for the intermediate values of U/t is generic—they exist in all three situations shown in Fig. 3. This confirms the trend observed in the earlier HF simulations in the intermediate coupling regime, where the vertical domain walls were found both for small doping $\delta \lesssim 0.08$ (see Ref. 6), and for the present doping level $\delta = 0.125$ (see Ref. 7).

Secondly, the correlation energy gives typically a substantial energy lowering. As it depends on the actual density distribution, it is thus different in various stripe phases. Therefore, the sequence of the obtained ground states in the LA method differs from that found in the HF calculation. At rather low values of U/t one finds the spin-bag phase both in the Hubbard model and in the Hubbard model with static phonons. This phase is characterized by rather small magnetic moments and therefore is stabilized by electron correlations. The particular correlation energy gain found for this solution supports the generic tendency towards phase separation into hole-rich and hole-poor regions already in the regime of $U/t \simeq 5$, and may be considered as a precursor effect to the formation of vertical stripes. The vertical nonmagnetic half-filled stripes [Fig. 2(a)] take over for larger values of U/t. They are robust and are stabilized by particularly large correlation energy gains at the nonmagnetic atoms in the broad range of U/t, while some other states with magnetic atoms on the walls are more stable at the HF level. This phenomenon is analogous to large correlation energy gains in the paramagnetic phase, known in itinerant magnetism.[14]

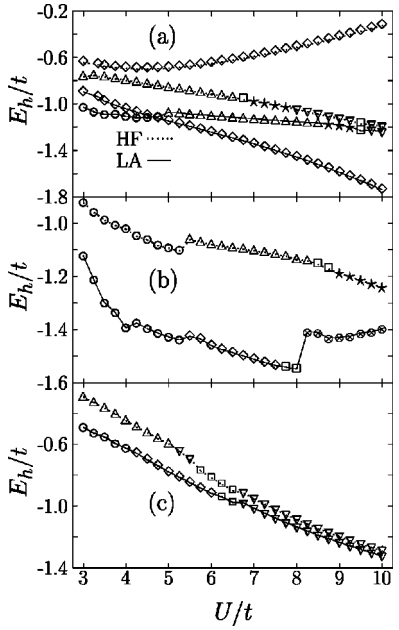

FIG. 3. Energy per one doped hole E_h/t (16) for various stripe phases found for 8×8 clusters at $\delta=0.125$ for increasing Coulomb repulsion U/t. The results of HF and LA calculations are shown by solid and dotted lines, respectively, for (a) Hubbard Hamiltonian (1), (b) Hubbard Hamiltonian with static phonons (2), (c) Hirsch Hamiltonian (3). In case (a) apart from the ground state structure also the locally stable states at higher energy are shown. Different symbols indicate various stripe phases: $\diamond$—nonmagnetic half-filled domain walls [Fig. 2(a)], $\otimes$—two alternating (01) domain walls [Fig. 2(b)], $\square$—vertical half-filled walls (with one hole per two atoms of the wall) [Fig. 2(c)], ∇—ordered polarons in the (11) direction corresponding to a grid of diagonally intersecting walls [Fig. 2(d)], $\star$—horizontal domain walls with quadrupling of charge and spin ordering (not shown), $\triangle$—magnetic half-filled domain walls (not shown), $\bigcirc$—spin-bag structure (not shown).

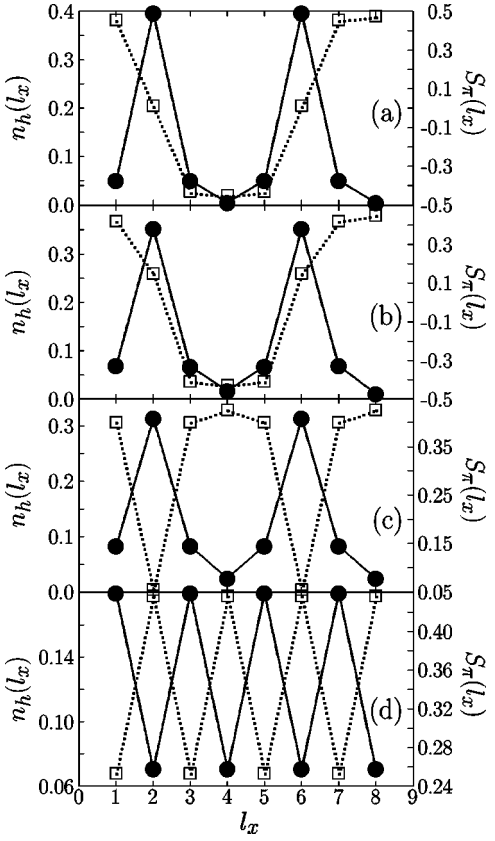

FIG. 4. Average doped hole density $n_h(l_x)$ (filled circles) and spin structure function $S_\pi(l_x)$ (open squares) as obtained for the most typical stripe phases found at $\delta=0.125$. Different panels correspond, respectively, to the solutions shown in Figs. 1(a)–(d).

Finally, the coupling to the lattice and the correlated hopping term in the Hirsch model results either in certain modifications of the vertical stripes, or in diagonal extended structures at large values of U/t. Local distortions due to static phonons stabilize the domain walls with magnetic moments on the walls for $U/t>7.5$. The same sequence of solutions as in the Hubbard model with phonons is also found in the Hirsch model, but here the spin-bag solution and the vertical half-filled walls [Fig. 2(a)] are almost degenerate in a range of small $U, 3<U/t<4.5$. In such a situation one might expect that one of these phases could be stabilized either by additional hopping elements to further neighbors, or by the coupling to the lattice. For $U/t>6.5$ one finds here the extended diagonal walls of Fig. 2(d).

The models (1) and (2) give quite similar results in the HF method,[7] with the same ground states moved to larger values of U/t in the presence of static phonons (Fig. 3). Such a change of the size of effective interaction follows from the enhancement of the local hopping elements on the bonds which connect the atoms at the domain walls with their nearest neighbors in the direction perpendicular to the wall due to lattice relaxation, effectively reducing the correlation effects. The opposite trend is observed in the Hirsch model (3), where the hopping elements in the regions of increased doped hole density are reduced, and the correlation effects are thus enhanced. Moreover, the magnetic moments (8) are here larger than in the Hubbard model for the same values of U/t. Therefore, the transition to the diagonal domain walls occurs for the Hirsch model at a much lower value of $U/t \simeq 6.5$ than in the Hubbard model, where such structures are found in the ground state only for $U/t>9.7$. We note that the same crossover is found in HF method applied to the Hubbard Hamiltonian at $U/t\simeq 7.7t$ which agrees well with the value of $U/t=8$ reported in the early study of Zaanen and Gunnarsson.[1]

Although the vertical half-filled domain walls are stable in a broad regime of intermediate values of U/t for the Hubbard model, without and with static phonons, we have found that the lines of enhanced doped hole density (7) may contain *magnetic* atoms, in contrast to the earlier HF studies,[1,6,7] where no magnetic moments were reported on the domain walls. This occurs in particular in the case of the Hirsch model at stronger interactions U [Figs. 1(c) and 1(d)], but such regions of enhanced doped-hole density occur then within a single AF domain, in contrast to the nonmagnetic and weakly magnetic structures which separate two different domains [see Figs. 1(a) and 1(b)].

The difference by a factor of 2 in the periodicity of charge and magnetic structures for the (01) half-filled domain walls which expresses the alternation of AF domains is shown in Figs. 4(a) and 4(b). The lines of increased hole density are accompanied by the reduced values of magnetization $S_\pi(l_x)$, and a change of phase in the AF order is found on the charge

TABLE I. Local charge density $n_{hi}=\langle 1-(n_{i\uparrow}+n_{i\downarrow})\rangle$ and local magnetization density $m_i=\frac{1}{2}|\langle n_{i\uparrow}-n_{i\downarrow}\rangle|$, for various stripe phases and parameters (U/t) of Fig. 1. Nonequivalent atoms in different textures are labelled according to the decreasing doped hole density.

stripe phase	i	$n_{hi,\mathrm{HF}}$	$n_{hi,\mathrm{LA}}$	$m_{i,\mathrm{HF}}$	$m_{i,\mathrm{LA}}$
Fig. 1(a)	1	0.379	0.396	0.000	0.000
	2	0.058	0.050	0.439	0.444
	3	0.005	0.004	0.462	0.463
Fig. 1(b)	1	0.468	0.523	0.082	0.090
	2	0.181	0.179	0.360	0.373
	3	0.149	0.127	0.354	0.380
	4	0.099	0.098	0.386	0.396
	5	0.052	0.038	0.414	0.427
	6	0.022	0.017	0.428	0.436
	7	0.014	0.007	0.447	0.453
Fig. 1(c)	1	0.440	0.445	0.242	0.247
	2	0.167	0.181	0.341	0.350
	3	0.112	0.119	0.367	0.377
	4	0.056	0.046	0.401	0.417
	5	0.028	0.024	0.413	0.423
Fig. 1(d)	1	0.455	0.455	0.263	0.265
	2	0.125	0.130	0.399	0.404
	3	0.119	0.122	0.404	0.409
	4	0.112	0.114	0.411	0.416
	5	0.033	0.025	0.451	0.458
	6	0.018	0.014	0.455	0.460
	7	0.013	0.010	0.455	0.460

walls. Such structures were observed in the experiments of Tranquada *et al.*,[3,4] and we conclude that the observed stripe phases might correspond either to nonmagnetic homogeneous walls [Fig. 2(a)], or to the walls with charge alternation [Fig. 2(b)]. In contrast, the remaining two structures shown in Fig. 1 are characterized by *the same periodicity* of the charge and magnetization distribution [see Figs. 4(c) and 4(d)]. Oscillation of both distributions along the (10) direction in the latter case is consistent with the diagonal character of the extended walls.

We have compared in Table I the charge (7) and the magnetization (8) density per site obtained in different phases shown in Fig. 1, as found in the HF and in the LA calculations (the HF values are defined here as the respective averages over the HF ground state). It is found that local correlations almost do not influence the density distribution and lead only to a slight increase of the magnetic moments. This behavior demonstrates that the leading on-site correlations give only small modifications of the ground state, increasing somewhat the differences between the charge density at the domain walls and within the undoped regions of the AF phase.

B. Overdoped systems, $\delta=0.25$

For the higher doping level $\delta=0.25$ somewhat different types of stripe phases are found. We present the typical stable solutions for increasing values of U/t in the panels (a)–(d) of Fig. 5, while some other structures found only in the HF ground states are shown in Fig. 6. First, the correlations stabilize a homogeneous phase at low U/t, and the spacially extended (broad) diagonal stripes along the (11) direction at larger values of $U/t\simeq 5$ (this is a different ground state than that obtained using the HF approximation). These qualitatively new states may be understood as follows.

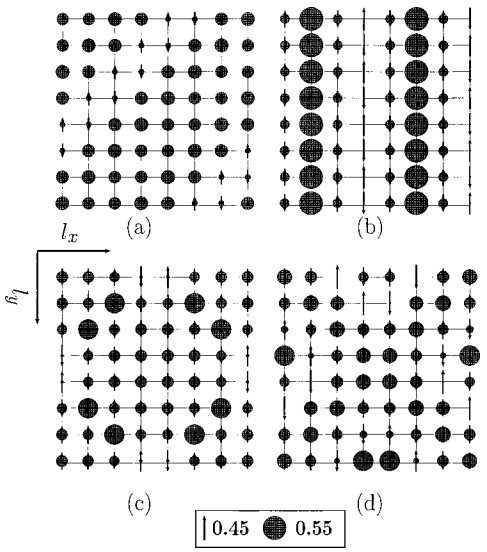

FIG. 5. The most typical stripe phases as obtained at doping $\delta=0.25$ using LA method: (a) two diagonal spacially extended domain walls with spin alternation ($U=6t$), (b) two filled (01) domain walls ($U=10t$), (c) ringlike domain wall with AF order ($U=7t$), (d) two diagonal extended walls intersecting each other ($U=10t$). The stripe phases (a) and (b) [(c) and (d)] were obtained in the Hubbard model with static phonons [Hirsch model]. The meaning of grey circles and arrows as in Fig. 1.

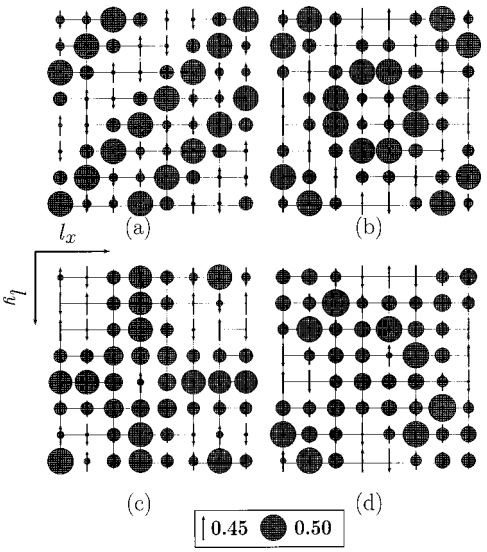

FIG. 6. Stripe structures found in the HF ground state at doping $\delta=0.25$, but destabilized by electron correlations within the LA method: (a) extended diagonal domain walls with spin alternation ($U=8.5t$), (b) ring of increased doped hole density in an AF domain ($U=10t$), (c) two walls intersecting each other in a single AF domain ($U=8t$), (d) two diagonal extended walls with locally increased hole density ($U=9.5t$). The stripe phases (a) and (b) [(c) and (d)] were obtained in the Hubbard model with [without] static phonons. The meaning of grey circles and arrows as in Fig. 1.

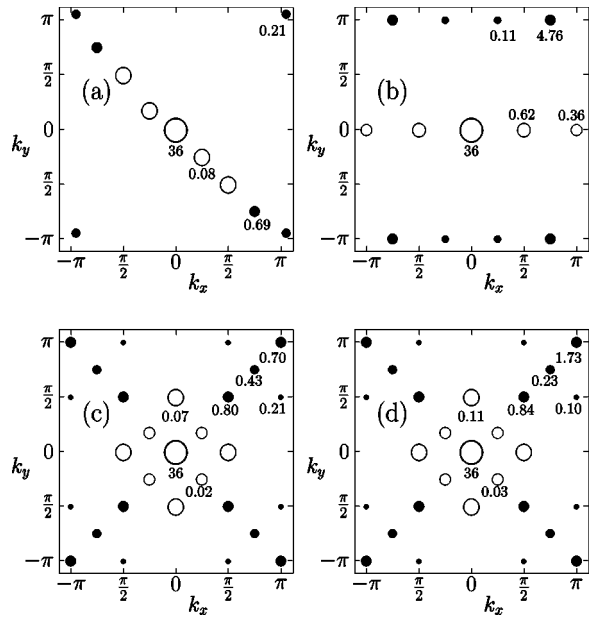

FIG. 7. The same as in Fig. 2, but for doping $\delta=0.25$. Different panels represent the most stable solutions shown in Fig. 5: (a) diagonal filled domain wall, $U=6t$ [Fig. 5(a)], (b) two filled (01) domain walls, $U=10t$ [Fig. 5(b)], (c) striped phase with a ring structure, $U=7t$ [Fig. 5(c)], (d) striped phase with two intersecting diagonal walls, $U=10t$ [Fig. 5(d)].

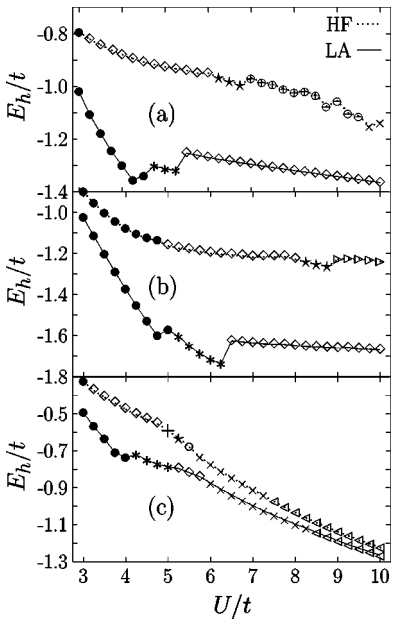

FIG. 8. Energy per one doped hole E_h/t for various stripe phases as obtained for 8×8 clusters at $\delta=0.25$ for increasing Coulomb repulsion U/t. The results of HF and LA calculations are shown by solid and dotted lines, respectively, for (a) Hubbard Hamiltonian (1), (b) Hubbard Hamiltonian with static phonons (2), (c) Hirsch Hamiltonian (3). Different symbols indicate various stripe phases: ●—homogeneous AF phase, *—diagonal (11) extended walls [Fig. 7(a)], ◇—filled nonmagnetic (01) domain walls [Fig. 7(b)], ×—fuzzy ringlike structures [Fig. 7(c)], ◁—filled vertical walls [Fig. 7(d)], ⋆—diagonal double walls [Fig. 6(a)], ▷—ring structure [Fig. 6(b)], ⊕—two walls intersecting each other [Fig. 6(c)], ⊖—two extended walls [Fig. 6(d)], +—extended ring structures [similar to that of Fig. 7(d)], ○—spin bag structure (not shown).

Under the tendency towards phase separation into hole-rich and hole-poor regions,[18,28] it is more difficult to accommodate the increased hole density in the vertical or horizontal stripes and therefore it appears to be easier to stabilize instead the broad diagonal stripes, either along the (11) direction alone, or intersecting domain walls along the (11) and $(\bar{1}1)$ direction (Fig. 5). The AF correlations are weaker at this level of doping (in comparison to these found for $\delta=0.125$), and except for the case of strong AF correlations in vertical (01) walls of Fig. 5(b), the reduced weak AF correlations survive only within the spacially extended domain walls [Figs. 5(a), 5(c), and 5(d)]. As in the case of $\delta=0.125$, increasing Coulomb interaction U/t suppresses the vertical nonmagnetic stripes and gives instead new extended structures, with all atoms being magnetic.

The extended domain walls [Fig. 7(a)] separate two AF domains and give the magnetic structure factor $S(\mathbf{k})$ with two distinct maxima at the $\mathbf{k}=(3\pi/4,-3\pi/4)$ and $(-3\pi/4,3\pi/4)$ points. This structure is, however, found only at relatively small values of $U/t\simeq5$ and is therefore not expected to emerge in an experiment. At higher values of U/t we have found again the vertical (01) *nonmagnetic domain walls* filled now by one hole per one wall atom [Fig. 7(b)]. Except for the increased doped hole density and somewhat reduced magnetic moments, this structure is qualitatively equivalent to two half-filled walls discussed above for the $\delta=0.125$ case [Fig. 2(a)], with strong magnetic maxima of $S(\mathbf{k})$ found again at the points $\mathbf{k}=(\pm3\pi/4,\pi)$.

The remaining two phases found in the overdoped systems ($\delta=0.25$; the LA method) show diagonal charge structures, and the corresponding magnetic and charge maxima are found both along the $(\bar{1}1)$ and the (11) direction [Figs. 7(c) and 7(d)], i.e., the intersecting diagonal walls with enhanced doped hole density. There is only a single AF domain, and thus strong maxima are found in $S(\mathbf{k})$ at the AF points $\mathbf{k}=(\pm\pi,\pm\pi)$. Having both charge $[C(\mathbf{k})]$ and magnetic $[S(\mathbf{k})]$ maxima at the same values of $\mathbf{k}$, the structures shown in Figs. 7(c) and 7(d) may be considered as a modification of the same phase with diagonal walls of increased density.

The complexity of the ground states found for the overdoped systems (at the doping of $\delta=0.25$) is best illustrated by the dependence of energy gain per one doped hole E_h/t on the Coulomb interaction U/t, shown in Fig. 8. A homogeneous solution with weak AF long-range order found at low values of U/t is replaced by several different stripe phases with increasing values of U/t. As expected, the onset of the stripe ordering occurs at higher values of U/t in the presence of electron correlations than in the HF calculation. Electron correlations contribute significantly to the stability of stripe phases, and stabilize in particular the filled vertical domain walls [Fig. 7(b)] at intermediate values of U/t. These structures were also found in the HF calculations in a range of smaller values of U/t for all three considered model Hamiltonians (1)–(3).

We have found the same qualitative trends when comparing three different models (1)–(3) as the trends found in the case of $\delta=0.125$, namely, (i) there is little difference between the Hubbard model without and with static phonons,

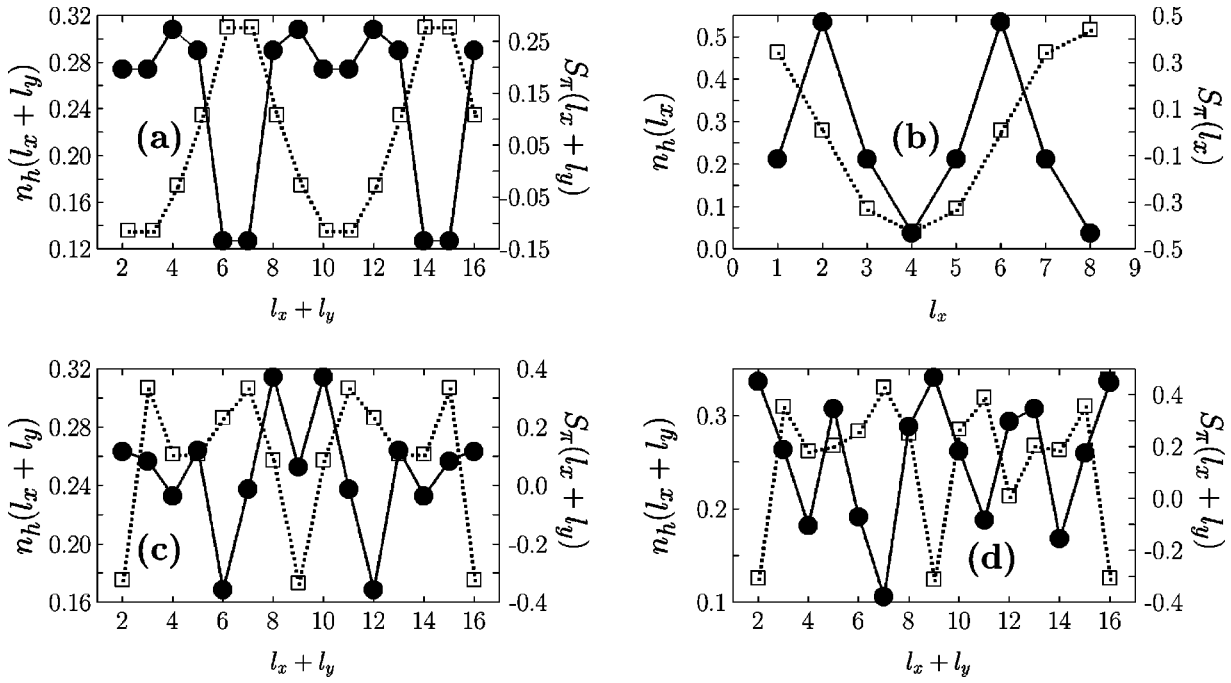

FIG. 9. Average doped hole density $n_h(l_x+l_y)[n_h(l_x)]$ (filled circles) and spin structure function $S_\pi(l_x+l_y)[S_\pi(l_x)]$ (open squares) as obtained for the stable solutions of Fig. 5.

except that the same stripe structures are stable at higher values of U in the latter case and (ii) the Hirsch Hamiltonian corresponds to a stronger coupling, and therefore the fuzzy-ring-like [Fig. 7(c)] and intersecting domain wall [Fig. 7(d)] structures occur here in a broad range of $6<U/t<10$, while the first of these structures is stable in the Hubbard model only above $U/t=10$. Somewhat surprisingly, the range of stability of the filled vertical walls [Fig. 7(b)] is much narrower ($5<U/t<6$) in the Hirsch model than in the Hubbard models, where such structures are favored in the regime corresponding to the cuprates, i.e., for $U/t>8$. This may suggest that the Hirsch Hamiltonian is less realistic model for the cuprates, in agreement with the published results concerning the mapping procedures from realistic multiband Hamiltonians (in cuprates) to simplified effective single band Hamiltonians.[21,29]

The charge and magnetic structures found in the overdoped regime (Fig. 9) are somewhat less symmetric than those found in the underdoped regime. Low doped hole density n_h (20) is accompanied by large magnetic moments (21) with AF nearest-neighbor correlations, resulting in large values of S_π. It is well seen in Figs. 9(a), 9(c), and 9(d) that the periodicity of magnetic structure is in these cases identical to that of the charge distribution; it involves half of the 8×8 cluster for two diagonal walls of Fig. 9(a), while it extends over the whole cluster in the remaining two cases. In contrast, the magnetic unit cell has a length of eight sites while the charge cell has a length of four sites for two vertical filled nonmagnetic stripes of Fig. 9(b). This result shows once again that this phase is physically equivalent to the vertical half-filled stripes found in the underdoped systems.

IV. DISCUSSION AND CONCLUSIONS

Summarizing, we have studied the stability of stripe phases in the Hubbard model without and with static phonons, and in the Hirsch model at two hole doping levels, $\delta=1/8$ and $\delta=1/4$, which correspond to the underdoped and overdoped cuprates. In both cases the stripe phases are more stable than the homegeneous solutions, indicating that the stripe ordering is generic and occurs always in doped AF Mott-Hubbard systems with intermediate Coulomb interaction U. The type of the stripe ordering, however, depends on the actual parameters and on the doping level.

We have found that electron correlations always increase the stability of the stripe phases, while the charge and magnetization distribution in a particular phase are only little modified by electron correlations with respect to those found in the HF approximation. Although the observed half-filled vertical stripes were found before in the HF calculations, they were unstable with respect to the filled walls and spiral phases.[7] Here we have found that electron correlations play a prominent role in stripe phases and *stabilize the observed half-filled domain walls* in the underdoped systems (at $\delta=1/8$). We emphasize that such solutions occur *without* any long-range Coulomb interaction which was recently shown to enhance the stability of half-filled domain walls within the Gutzwiller ansatz.[9] The most stable stripe phase obtained in these systems has the expected alternating AF domains separated by nonmagnetic domain walls, as observed experimentally. Interestingly, the half-filled stripes absorb more holes with increasing doping beyond $\delta=1/8$, and give still the same form of $S(\mathbf{k})$ for the doping of $\delta=1/4$, in qualitative agreement with the observed[5] broad plateau in the shift of the maxima of $S(\mathbf{k})$, found at $\mathbf{k}=[(1\pm2\eta)\pi,\pi]$, with $\eta=1/8$ in both cases, with respect to the AF peak found at $\mathbf{k}=(\pi,\pi)$.

The present method gives also that the nonmagnetic half-filled walls are more stable at $\delta=1/8$ in the regime of intermediate values of U/t than any of the other textures, including the bond-centered domain walls found in the DMRG

calculations,[8] pointing out that the accurate treatment of correlation effects is crucial for a better understanding of the ground states in doped antiferromagnets. However, the answer obtained in the present study concerning the instability of bond-ordered stripes obtained in the DMRG calculations by White and Scalapino[8] with respect to the site-ordered stripes might not be final. The ansatz for the correlated ground state (5) does not include two important effects: (i) the spin-spin correlations between nearest neighbors and (ii) the one-particle excitations which optimize the charge distribution in nonhomogeneous systems.[30] It may be expected that both types of correlations would decrease the energy difference between the bond-ordered and site-ordered stripes, and might stabilize the former. Moreover, the quantum fluctuations which go beyond the present treatment are expected to be large in bond-ordered stripes,[31] and they might stabilize such structures. Further studies are needed to clarify under which circumstances the bond-ordered stripes could form in the ground state.

Finally, we did not address here the consequences of the extended hopping to second (t') and third (t'') neighbors. As these elements are small as in $La_{2-x}Sr_xCuO_4$,[21,29] we expect that the vertical nonmagnetic stripes obtained in the present study are the most stable structures in the relevant regime of U/t. However, for stronger next-neighbor hoppings t' and t'', as found for doped Y and Bi superconductors,[21,29] there are indications that the stripe structures are more spacially extended and are diagonal, as obtained also within the DMFT method,[10] or even can evaporate and so enhance $d_{x^2-y^2}$ pairing correlations.[32] If confirmed, this would explain (i) why it is so difficult to observe static stripes in these two classes of high-temperature superconductors and (ii) why their superconducting transition temperatures are so much higher than those of La superconductors.

Summarizing, we have found nonmagnetic (01) domain walls within the most stable stripe phases with a charge unit cell consisting of four atoms at $\delta=1/8$ and $\delta=1/4$, and qualitatively the same magnetic response $S(\mathbf{k})$ in neutron scattering experiments. Our results show that the short-range (on-site) Coulomb interactions alone suffice to stabilize the stripe phases and thus explain the physical origin of the stripes.[33] It is likely that such stripe phases as found in the present paper are metallic,[10,17] but this question could be answered only in a dynamical approach. We believe that the present results motivate further search for more accurate description of change and magnetic ordering in stripe phases, and for a better understanding of the interplay between magnetic and charge degrees of freedom in doped Mott insulators.

ACKNOWLEDGMENTS

It is our pleasure to thank J. Zaanen for many stimulating discussions, and M. Fleck and A. Georges for valuable comments. We acknowledge the support by the Committee of Scientific Research (KBN) of Poland, Project No. 2 P03B 175 14.

APPENDIX: TREATMENT OF STATIC PHONONS

The single-band Hubbard Hamiltonian with added Peierls coupling between the electrons and the (static) lattice distortions was used in Ref. 7 as a possible model which might support the formation of stripe phases in the cuprates. At $U=0$ this Hamiltonian reduces to the Su-Schriffer-Heeger model[22] which was applied with great success to explain the dimerization of polyacetylene. Originally, the Su-Schriffer-Heeger Hamiltonian was introduced for a homogeneous system (with the same charge at each lattice site), and under a constraint that the sum of neighboring bond dilatations and elongations is zero. This condition is absent in the present model,[7] and the lattice contracts. The energy minimum in the HF approximation was found by using an iterative procedure (until self-consistency) in Ref. 7. Thereby, an approximate saddle-point formula for the phonon field was used which relates the actual contraction of a given bond u_{ij} to the bond charge density $\langle c^\dagger_{i\sigma}c_{j\sigma}\rangle$,

$$u_{ij}\simeq-\frac{\alpha t}{K}\sum_\sigma\langle c^\dagger_{i\sigma}c_{j\sigma}\rangle. \tag{A1}$$

The averages $\langle c^\dagger_{i\sigma}c_{j\sigma}\rangle$ do depend on the actual bond length, but the individual bonds are treated as independent from each other. Although this procedure works well in the HF approximation,[7] there is no guarantee that it will work in exact ground state. Therefore, we have introduced a more accurate procedure which consists of two steps as described below.

First we consider that the doping δ is reasonably small so that we are quite close to the half-filled case. The AF ground state at half-filling is used to establish the reference bond length in the presence of electron-phonon coupling. This state is homogeneous and the minimum is given by a single variable, i.e., $u_{ij}=u^0$ for each pair of nearest neighbors i and j.

As a second step we perform a Taylor expansion (up to second order) of all the HF averages around the reference solution found at half filling. It may be expected that one is still close enough to the real global minimum at not too high doping δ, and the linear correction to u^0 will suffice. As the first average quantity one has to expand the bond charge density $\langle c^\dagger_{i\sigma}c_{j\sigma}\rangle$ which determines the kinetic energy, used before in Eq. (A1), assuming that the local approximation applies in leading order

$$\langle c_{i\sigma}c_{j\sigma}(\{u_{rs}\})\rangle\approx\langle c_{i\sigma}c_{j\sigma}(u^0)\rangle+c_1\delta u_{ij}+c_2\delta u_{ij}^2+\cdots, \tag{A2}$$

where $\delta u_{ij}=u_{ij}-u^0$ is the change of the bond length with respect to the half-filled case. The unknown expansion coefficients c_1 and c_2 can be obtained without any difficulty by a straightforward numerical differentiation. Note, however, that any other terms with δu_{rs}, such that $\{rs\}\neq\{ij\}$, are ignored. Therefore, this local approximation may work or not, and its validity has to be checked *a posteriori*.

In order to evaluate the total energy (9) one has to determine an average double occupancy normalized per one site, $(1/N)\Sigma_i\langle n_{i\uparrow}n_{i\downarrow}(\{u_{rs}\})\rangle$. This quantity is invariant with respect to the translations of the lattice origin. This means that there are only two expansion coefficients, d_1 and d_2, to be fixed using numerical differentiation

$$\sum_i \langle n_{i\uparrow} n_{i\downarrow}(\{u_{rs}\})\rangle \approx \sum_i \langle n_{i\uparrow} n_{i\downarrow}(u^0)\rangle + d_1 \sum_{ij} \delta u_{ij} + d_2 \sum_{ij} \delta u_{ij}^2 + \cdots . \quad \text{(A3)}$$

The diagonal quadratic terms as written above are not the only possible ones, but we have chosen here once again the simplest formula using a local expansion. Its validity has to be checked once again after completing the minimization procedure.

By inserting the Taylor expansions (A2) and (A3) into the HF Hamiltonian H_{HF}, and minimizing the total energy $E_{\mathrm{HF}} = \langle H_{\mathrm{HF}} \rangle$ over δu_{ij}, one obtains an analytic solution by solving a set of uncoupled quadratic equations. We have taken a simplifying assumption that the same bond contractions $\{\delta u_{ij}\}$ as in the HF approximation minimize the energy in correlated states. As the distortions δu_{ij} depend primarily on the bond hole density (A2), we have found that they may be determined with sufficient accuracy using the HF states.

In order to trust the present procedure one has to verify whether (i) the first order term $\propto d_1$ is indeed dominant with respect to the higher order $\propto d_2$ term and (ii) the derived set of ''semianalytic'' δu_{ij} indeed lowers the HF energy, i.e., whether $E_{\mathrm{HF}}(\{u_{ij}\}) < E_{\mathrm{HF}}(u_0)$. We have completed these checks and found positive answers to both of the above questions. This justifies our approximate procedure which uses the Taylor expansions (A2) and (A3) and allows us to obtain conclusive results from the Hubbard Hamiltonian with static phonons (2). We have also verified that the obtained minimum is close to the approximate saddle-point relations (A1).

[1] J. Zaanen and O. Gunnarsson, Phys. Rev. B **40**, 7391 (1989).

[2] T.E. Mason, G. Aeppli, and H.A. Mook, Phys. Rev. Lett. **65**, 2466 (1990); S.-W. Cheong, G. Aeppli, T.E. Mason, H. Mook, S.M. Hayden, P.C. Canfield, Z. Fisk, K.N. Clause, and J.L. Martinez, *ibid.* **67**, 1791 (1991).

[3] J.M. Tranquada, B.J. Sternlieb, J.D. Axe, Y. Nakamura, and S. Uchida, Nature (London) **375**, 561 (1995); J.M. Tranquada, J.D. Axe, N. Ichikawa, Y. Nakamura, S. Uchida, and B. Nachumi, Phys. Rev. B **54**, 7489 (1996).

[4] J.M. Tranquada, J.D. Axe, N. Ichikawa, A.R. Moodenbaugh, Y. Nakamura, and S. Uchida, Phys. Rev. Lett. **78**, 338 (1997).

[5] K. Yamada, C.H. Lee, Y. Endoh, G. Shirane, R.J. Birgeneau, and M.A. Kastner, Physica C **282-287**, 85 (1997).

[6] D. Poilblanc and T.M. Rice, Phys. Rev. B **39**, 9749 (1989); H.J. Schulz, Phys. Rev. Lett. **64**, 1445 (1990); T. Giamarchi and C. Lhuillier, Phys. Rev. B **42**, 10 641 (1990); M. Inui and P. Littlewood, *ibid.* **44**, 4415 (1991); J. Zaanen and Littlewood, *ibid.* **50**, 7222 (1994).

[7] J. Zannen and A.M. Oleś, Ann. Phys. (Leipzig) **5**, 224 (1996).

[8] S.R. White and D.J. Scalapino, Phys. Rev. Lett. **80**, 1272 (1998); **81**, 3227 (1998).

[9] G. Seibold, C. Castellani, C. Di Castro, and M. Grilli, Phys. Rev. B **58**, 13 506 (1998).

[10] A. I. Lichtenstein, M. Fleck, A. M. Oleś, and L. Hedin, J. Supercond. (to be published).

[11] J.M. Tranquada, D.J. Buttrey, V. Sachan, and J.E. Lorenzo, Phys. Rev. Lett. **73**, 1003 (1994); V. Sachan, D.J. Buttrey, J.M. Tranquada, and J.E. Lorenzo, Phys. Rev. B **51**, 12 742 (1995).

[12] G. Stollhoff and P. Fulde, J. Chem. Phys. **73**, 4548 (1980); G. Stollhoff, *ibid.* **105**, 227 (1996).

[13] G. Stollhoff and P. Thalmeier, Z. Phys. B **43**, 13 (1981); A.M. Oleś, Phys. Rev. B **23**, 271 (1981); J. Dutka and A.M. Oleś, *ibid.* **42**, 105 (1990); **43**, 5622 (1991).

[14] A.M. Oleś and G. Stollhoff, Phys. Rev. B **29**, 314 (1984); G. Stollhoff, A.M. Oleś, and V. Heine, *ibid.* **41**, 7028 (1990).

[15] P. Fulde, *Electron Correlations in Molecules and Solids*, Vol. 100 of *Springer Series in Solid State Sciences* (Springer Verlag, Berlin, 1991).

[16] H. Eskes, O.Y. Osman, R. Grimberg, W. van Sarlos, and J. Zaanen, Phys. Rev. B **58**, 6963 (1998).

[17] J. Zaanen, O.Y. Osman, and W. van Saarloos, Phys. Rev. B **58**, R11 868 (1998).

[18] V.J. Emery and S.A. Kivelson, Physica C **209**, 597 (1993); M.I. Salkola, V.J. Emery, and S.A. Kivelson, Phys. Rev. Lett. **77**, 155 (1996).

[19] R. Micnas, J. Ranninger, and S. Robaszkiewicz, Phys. Rev. B **39**, 11 653 (1989).

[20] J.E. Hirsch, Phys. Lett. A **136**, 163 (1989); Phys. Rev. B **48**, 3327 (1993).

[21] J.H. Jefferson, H. Eskes, and L.F. Feiner, Phys. Rev. B **45**, 7959 (1992); L.F. Feiner, J.H. Jefferson, and R. Raimondi, *ibid.* **53**, 8751 (1996); R. Raimondi, L.F. Feiner, and J.H. Jefferson, *ibid.* **53**, 8774 (1996).

[22] W.P. Su, J.R. Schrieffer, and A.J. Heeger, Phys. Rev. B **22**, 2099 (1980).

[23] B.J. Alder, K.J. Runge, and R.T. Scaletter, Phys. Rev. Lett. **79**, 3002 (1997).

[24] A. Dobry, A. Greco, J. Lorenzana, and J. Riera, Phys. Rev. B **49**, 505 (1994).

[25] M.C. Gutzwiller, Phys. Rev. **137**, A1726 (1965); D. Vollhardt, Rev. Mod. Phys. **56**, 99 (1984).

[26] An alternative formulation with a single Slater determinant is required for mixed-spin one-particle eigenstates, as for instance in spin-spiral states. Such wave functions lead to severe technical complications in the calculation of correlated states. It follows from the earlier numerical studies[6–10] that the stripe phases have lower energy than spin spirals and therefore the latter states were not considered.

[27] W. Jones and N. H. March, *Theoretical Solid State Physics*, Vol. XXVII, *Interscience Monographs and Texts in Physics and Astronomy*, edited by R. E. Marshak (Wiley, London, 1973).

[28] E. Dagotto, Rev. Mod. Phys. **66**, 763 (1994).

[29] O.K. Andersen, J. Phys. Chem. Solids **59**, 1769 (1998).

[30] A.M. Oleś, F. Pfirsch, P. Fulde, and M. C. Böhm, J. Chem. Phys. **85**, 5183 (1986).

[31] J. Tworzydło, O.Y. Osman, C. van Duin, and J. Zaanen, Phys. Rev. B **59**, 115 (1999).

[32] S.R. White and D.J. Scalapino, Phys. Rev. B **60**, R753 (1999).

[33] J. Zaanen, J. Phys. Chem. Solids **59**, 1769 (1998).